



OPEN

SUBJECT AREAS:
ELECTRONIC PROPERTIES
AND MATERIALS
NANOPARTICLESReceived
8 July 2014Accepted
8 December 2014Published
8 January 2015Correspondence and
requests for materials
should be addressed to
C.B. (cbsp@uohyd.
ernet.in)

Inter-cluster distance dependence of electrical conduction in nanocluster assembled films of silver: a new paradigm for design of nanostructures

Chandrabhas Bansal¹, S. G. Praveen², J. T. T. Kumaran² & Ashok Chatterjee¹¹School of Physics, University of Hyderabad, Hyderabad 500046, India, ²Department of Physics, N. M. Christian College, Marthandam, 629165, India.

The transport properties of films assembled from metal nanoclusters can be significantly different from the metals in their bulk or thin film forms due to quantum confinement effects and several competing energy and length scales. For a film composed of metal nanoclusters as its building blocks, the cluster size and the inter-cluster separation are parameters that can be varied experimentally. Here we show that the electrical conductivity of a film composed of silver nanoclusters can be changed by 9 orders of magnitude as a function of the average inter-cluster separation while keeping the average cluster size same. For inter-cluster separations of 9 nanometres or more the conductivity is insulating type whereas for lesser inter-cluster separations the conductivity behaviour is metallic type with a positive temperature coefficient of resistance. In the intermediate range between the two regions, a very interesting temperature-independent conductivity is seen. Our work provides a new paradigm for design of artificial solid structures composed of nanoclusters. The properties of these nanostructures could be tuned by varying the inter-cluster distances to get the desired properties in the same material.

There have been several transport measurements in granular metals, doped systems of self-assembled germanium quantum dots and on Cd-Se nanocrystalline thin films^{1–11}. In this work we report for the first time a systematic investigation of the effect of varying the inter-cluster separation on the properties of a quasi-two dimensional monolayer of nanoclusters of silver. We would like to stress that these nano cluster assembled films are different from the previously studied granular metal films^{1–6} which consist of crystallite grains separated by grain boundaries. In our system the nanoclusters are pre-formed in an agglomeration zone after sputtering and are subsequently deposited on a substrate. The microstructure thus consists of isolated nanoclusters without grain boundaries and separated by an average inter-cluster distance that depends on the deposition time.

The details of the cluster deposition methods, structural characterization and measurement techniques are described in the Experimental Methods section at the end of this manuscript. The representative Field Emission Scanning Electron Microscope (FESEM) images of the as-deposited nanocluster films deposited for various periods of time are shown in figure 1 together with the size distribution of clusters. The variation of average inter-cluster separation is shown in figure 2 as a function of the deposition time. This was modelled with the Dose–Response formula¹²,

$$s = s_1 + (s_2 - s_1) / [1 + 10^{(\log t_0^{-1} - t)^p}] \quad (1)$$

Here s_1 and s_2 are the lower and upper asymptotic limits of the inter cluster separation (s), p is an exponent, t is the deposition time and t_0 is the time at which the value of s goes to a value halfway between s_1 and s_2 . This formula is applicable to biological systems to describe the effect of the dose of a stressor (such as pollutant, drug or radiation) on the receptor (such as organism). In our system the dose of the clusters is proportional to the deposition time and the inter-cluster separation measures the response to the deposition of clusters on the substrate. Our data could be fitted with this behaviour with $p = -7.7$ and a t_0 value of 10 minutes. Corresponding to this deposition time the inter-cluster separation is 9 nm as seen from figure 2. The measured

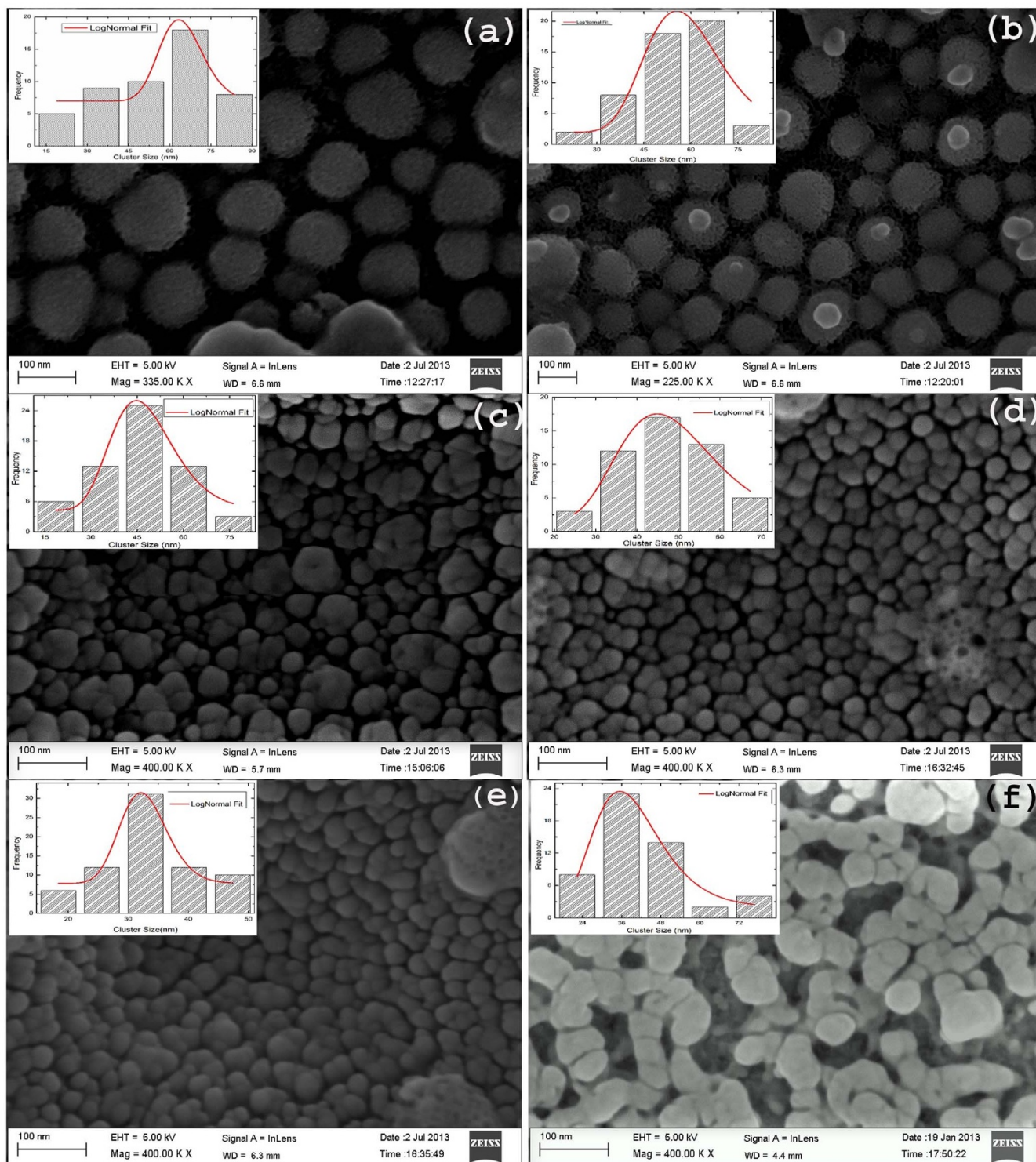


Figure 1 | FESEM images of as-deposited Ag nanocluster films for different deposition times: (a) 7.5 minutes (b) 9 minutes (c) 11.5 minutes (d) 12 minutes (e) 15 minutes and (f) 20 minutes. For images (a) and (b) a thin gold layer was deposited on the samples to avoid charging effects. The thin wire like projections seen on the clusters in these images are because of gold deposition. The insets of the micrographs show the size distribution of clusters estimated using ImageJ software.

resistance showed a negative temperature coefficient for nanocluster deposition times of up to 9 minutes and a positive temperature coefficient for deposition times of 12 minutes or more. Between these two regions of conduction the resistance showed a temperature independent behaviour. The representative data for the temperature dependence of resistance is shown in figure 3 for some deposition times.

Our system of nanocluster assembled films can be modelled as a two dimensional system of conducting islands separated by non-conducting regions. In the limit of large separation between the conducting metallic clusters the conduction is insulating type. As the cluster density increases, a critical percolation threshold is reached when there is a continuous conducting path for the carrier transport. A percolation radius r_c is defined in terms of the parameter

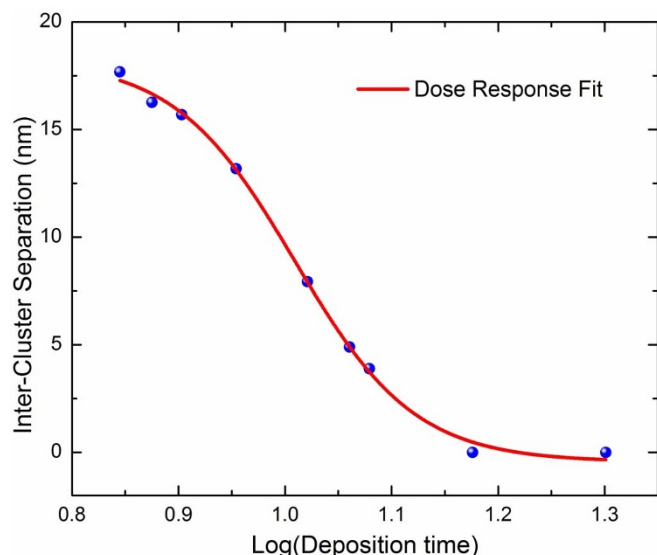


Figure 2 | Measured average inter cluster separation versus deposition time. The solid line is a fit to the data using the dose-response formula.

B_c which for a two dimensional system is defined as¹³:

$$B_c = \pi N r_c^2 \quad (2)$$

where N is the average number of sites per unit area. The parameter B_c represents the mean number of bonds per site. Different estimates of B_c give values in the range 4.5 to 3.2 for this parameter¹⁴ with an average value of 4.1. A comparison with experimental data can be made by estimating the areal fraction (θ_c) of the conducting islands at the percolation threshold. This can be calculated using the critical parameter B_c for a two dimensional system as shown by Zallen and Scher¹⁵, and is given by

$$\theta_c = 1 - \exp(-B_c/4) \quad (3)$$

For $B_c = 4.1$, one gets a critical areal fraction $\theta_c = 0.64$.

Experimentally we have obtained a critical value of average inter-cluster separation of 9 nm at which the conductivity changes from insulating to metallic. The average cluster size is 50 nm. The areal fraction of conducting islands in the form of disks of average radius R embedded in a rectangle of sides $2(R+r)$ would be $\pi R^2/4(R+r)^2$ where $2r$ is the inter-cluster separation. The estimated occupied areal fraction for the average radius and inter-cluster separation given

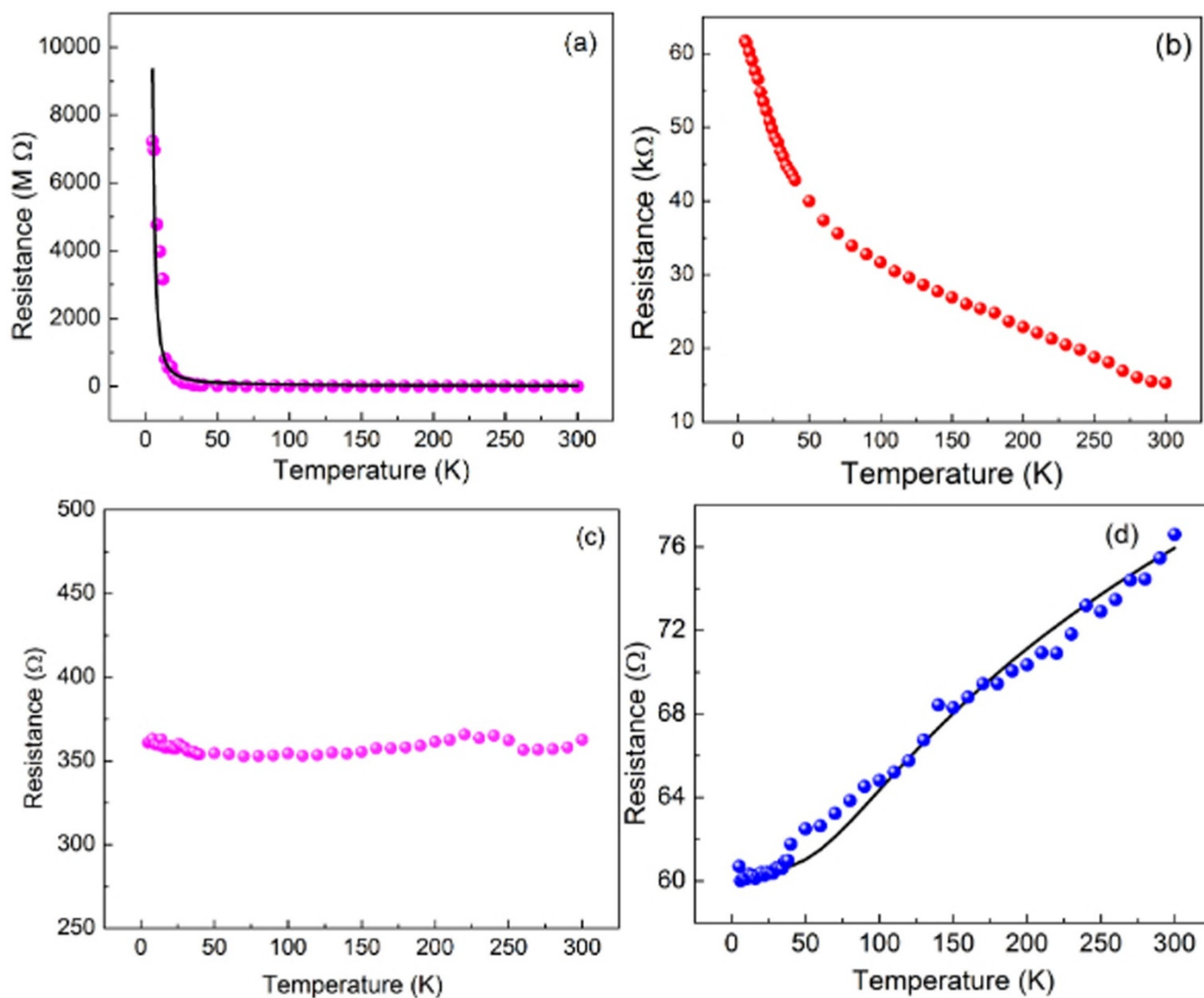


Figure 3 | The temperature dependence of channel resistance for deposition times of (a) 7.5 min (b) 9 min (c) 11.5 min and (d) 12 min. The data for 7.5 minutes was fitted to the Efros-Shklovskii model and the data for 12 minute deposition time was fitted to the Bloch-Grüneisen formula.

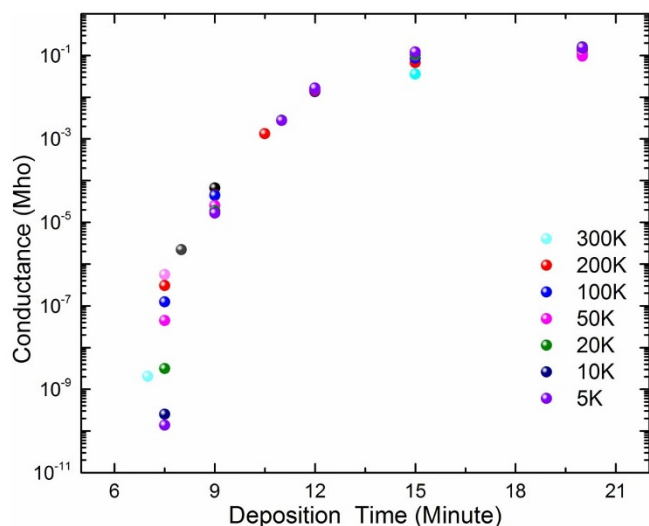


Figure 4 | The dependence of electrical conductance of silver nanocluster films on deposition time at different temperatures. The points at all temperatures lie on a universal plot showing the same underlying mechanism for conductivity change viz. the variation of inter-cluster separation with deposition time.

above comes out to be 0.56 in rough agreement with the calculated value of 0.64 from model calculations. It may be mentioned here that the value of inter-cluster separation of 9 nm that we have taken for these estimates corresponds to the deposition time value that gives an inter-cluster separation half way between the asymptotic values of this quantity. This value can depend on the model chosen to fit the data and hence this estimate of areal fraction is approximate. However it does not change the basic result that there is a critical areal fraction of area occupied by the clusters below and above which the conduction behaviour is different.

In figure 4 we have plotted the variation of conductance at different temperatures as a function of deposition time. There is change of conductivity by nine orders of magnitude. Interestingly all the data fall on a universal curve suggesting that the conductivity variation is indeed due to an intrinsic variation of average cluster-cluster separation with deposition time.

In the metallic regime the Bloch-Grüneisen equation was used to describe the temperature dependence of resistance, whereas in the insulating regime the Efros-Schlovskii variable range hopping model fitted the data reasonably well. However the intermediate region between the two regions a new and unusual temperature independent conductivity was observed as shown in figure 3c. A possible explanation of the unusual temperature independent conduction in the intermediate region can be given using the theoretical models developed by Ambegaonkar et al¹⁶ and by Miller and Abrahams¹⁷. The Fermi levels of electrons for individual clusters would lie at approximately the same energies as we move from an insulating to the metallic state when the electronic wave functions of the clusters start overlapping and create a band with electrons filled up to a single Fermi level. The tunnelling of electrons lying at the Fermi level of the individual clusters would be responsible for a temperature independent conductivity since the tunnelling would be independent of temperature between energy levels lying at the same energy as shown by the authors^{16,17} mentioned above.

Photo induced current was also observed for the nanocluster films. Figure 5 shows the measured IV characteristics of a film deposited for 11 minutes as a function of optical power from a halogen lamp. We see a current increase of almost 50 per cent over a very small area of 0.2 mm². The work function of a metal has been observed to increase with decrease in size¹⁸, so the observed current increase cannot be

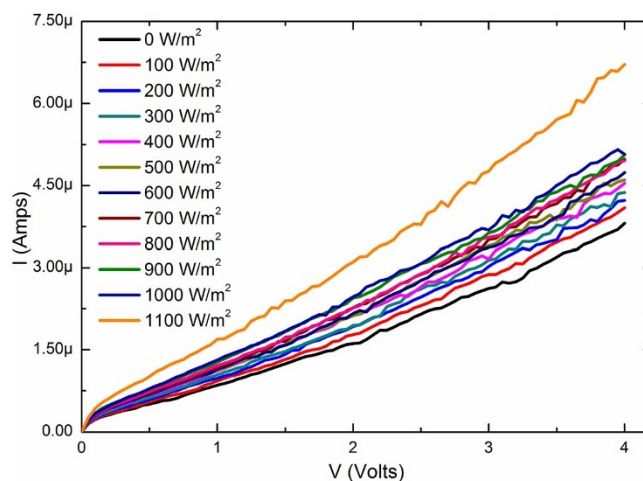


Figure 5 | IV characteristics of the 11 minute deposited film as a function of the light intensity from a halogen lamp.

attributed to a photoelectric effect. The increase in current can be attributed to an increase in tunnelling between nanoclusters due to excitation of electrons to higher energy levels and an increased tunnelling probability.

In conclusion, we have shown that the properties of nanocluster films could be controlled by varying the inter cluster separation. The conductivity of silver nanocluster films could be changed by nine orders of magnitude as a function of the inter cluster separation. The temperature dependence of conductivity was governed by variable range hopping in the insulating state and by metallic conduction in the metallic state. In the intermediate range there was an unusual temperature-independent conduction over a wide temperature range of 5 K–300 K. Such a material could find applications in designing of electronic devices, sensors and circuits that need to function over an extended temperature range. Our work provides a new paradigm for designing solids of the same metal with the desired electronic properties. This approach can be extended to design artificial solids in three dimensions or thicker nanocluster films by forming layers of two dimensional nanocluster films of a specified inter-cluster separation with a layer of insulator of the same thickness as the inter-cluster separation or by controlled co-deposition of clusters of a metallic and insulating material to get the desired inter cluster separation. We thus have a new paradigm for making tunable nanostructures.

Experimental Methods

The substrate was a commercially available Indium Tin Oxide (ITO) coated Polyethylene Terephthalate (PET) flexible substrate with a surface resistivity of 100 Ω/sq. An oxide (HfO₂) layer of thickness 80 nm was deposited on the substrate by RF sputtering. The sputtering deposition was carried out at a working pressure of 4.5×10^{-3} torr and a magnetron power of 60 Watts. Before depositing silver nanoclusters a self-assembled monolayer (SAM) of Trichlorocyclohexyle Silane (TCCHS) was made on the oxide by spin coating. The spin coating was carried in a glove box (Model MB20 G glove box from MBraun with O₂ and H₂O level maintained at less than 0.1 ppm). It was observed that the concentrations of TCCHS in Toluene and rotation speed of the spin coater were important parameters and these were optimized to get a uniform film. These parameters were found to be 1 mM and 5000 rpm respectively. Two contact electrodes of thickness 100 nm were formed by vacuum deposition of Silver (Ag) metal on the SAM. The channel between the electrodes was formed by using a 0.17 mm diameter gold wire as shadow mask. A base pressure of 5×10^{-6} torr and working pressure of 7×10^{-4} torr was kept during the vacuum evaporation process. The channel length was 100 micrometre and channel width was 2 mm.

Silver Nano Clusters were deposited using a Nanocluster Deposition System (Model Nanodep60 from Oxford Applied Research, UK). In this system, atoms of the target material get sputtered by a dc magnetron and move in an agglomeration chamber along with a carrier argon gas of 99.99% purity. Nanoclusters are formed in this chamber and are made to go through an aperture into a deposition chamber that is maintained at a slightly lower pressure than the agglomeration chamber. The distance between the substrate and apertures was 55 cm. The base pressure achieved



in system before the start of deposition was 7×10^{-7} Torr and a working pressure of 5×10^{-5} Torr was obtained during the aggregation gas flow whose flow rate was maintained at 100 sccm. The current in the DC magnetron was held constant at 0.2 A and the power level was about 75 Watts. The nanoclusters were deposited for different durations of time ranging from 7 min to 20 min in order to achieve different inter-cluster distances. For small deposition times the cluster separation was large and it decreased with increase in deposition time. The micro structural characterization of the films was done using a Field Emission Scanning Electron Microscope (Model Ultra55 from Carl Zeiss, Germany). The operating voltage of FESEM used was 5 KV with a working distance of 4–5 mm.

Current versus voltage (IV) measurements were carried out using a Semiconductor device analyzer (Agilent B1500 A) equipped with three source measure units (SMU). Two of the SMU's were high resolution units whereas one of them was a high power unit. The temperature of the samples was varied in the range 5 K–300 K using a Cryogenic Probe Station (Model CRX-4K from Lake Shore Cryotronics). The temperature inside the probe station was controlled by two temperature controllers (Lakeshore Model 336), one of them near the sample and the other at the cold head. The conductance of the samples was deduced from the slopes of the IV curves.

- Sheng, P., Abeles, B. & Arie, Y. Hopping conductivity in granular metals. *Phys. Rev. Lett.* **31**, 44–47 (1973).
- Abeles, B., Sheng, P., Coutts, M. D. & Arie, Y. Structural and electrical properties of granular metal films. *Adv. Phys.* **24**, 407–461 (1975).
- Barzilai, S., Goldstein, Y., Balberg, I. & Helman, J. S. Magnetic and transport properties of granular cobalt films. *Phys. Rev. B* **23**, 1809–1817 (1981).
- Savvides, N., McAlister, S. P. & Hurd, C. M. Electrical conduction in granular Cu-SiO₂ films. *Can. J. Phys.* **60**, 1484–1489 (1982).
- Simon, R. W., Dalrymple, B. J., Van Vechten, D., Fuller, W. W. & Wolf, S. A. Transport measurements in granular niobium nitride cermet films. *Phys. Rev. B* **36**, 1962–1968 (1987).
- Gerber, A., Milner, A., Deutscher, G., Karpovsky, M. & Gladkikh, A. Insulator-superconductor transition in 3D granular Al-Ge films. *Phys. Rev. Lett.* **78**, 4277–4280 (1997).
- Murawski, L. *et al.* The electronic conductivity mechanism in Bi-Sr-Ca-Cu-O glass-ceramics. *Philos. Mag. B* **80**, 1093–1103 (2000).
- Yakimov, A. I. *et al.* Long-range Coulomb interaction in arrays of self-assembled quantum dots. *Phys. Rev. B* **61**, 10868–10876 (2000).
- Yakimov, A. I., Dvurechenskii, A. V., Nikiforov, A. I. & Bloshkin, A. A. Phononless hopping conduction in two-dimensional layers of quantum dots. *JETP Lett.* **77**, 376–380 (2003).
- Moreira, H. *et al.* Electron co-tunnelling transport in gold nanocrystal arrays. *Phys. Rev. Lett.* **107**, 1–5 (2011).
- Beloborodov, I. S., Lopatin, A. V., Vinokur, V. M. & Efetov, K. B. Granular electronic systems. *Rev. Mod. Phys.* **79**, 469–518 (2007).

- Seefeldt, S. S., Jensen, J. E. & Fuerst, E. P. Log-logistic analysis of herbicide dose response relationships. *Weed Technology* **9**, 218–227 (1995).
- Shklovskii, B. I. & Efros, A. L. *Electronic Properties of Doped Semiconductors* (Springer-Verlag, Berlin, 1984).
- Pike, G. E. & Seager, C. H. Percolation and conductivity: a computer study. *J. Phys. Rev. B* **10**, 1421–1434 (1974).
- Zallen, R. & Scher, H. Percolation on a continuum and the localization-delocalization transition in amorphous semiconductors. *Phys. Rev. B* **4**, 4471–4479 (1971).
- Ambegaoankar, V., Halperin, B. I. & Langer, J. S. Hopping conductivity in disordered system. *Phys. Rev. B* **4**, 2612–2620 (1971).
- Miller, A. & Abrahams, E. Impurity conduction at low concentrations. *Phys. Rev.* **120**, 745–755 (1960).
- Zhou, L. & Zachariah, M. Size resolved particle work function measurement of free nanoparticles: Aggregates vs. Spheres. *Chemical Physics Letters* **525–526**, 77–81 (2012).

Acknowledgments

One of the authors (C. Bansal) would like to thank the Department of Science and Technology for support under the PURSE program and also under Project No. SR/S2/CMP-054/2006.

Author contributions

C.B. and S.G.P. wrote the manuscript, J.T.T.K. and A.C. reviewed the manuscript.

Additional information

Competing financial interests: The authors declare no competing financial interests.

How to cite this article: Bansal, C., Praveen, S.G., Kumaran, J.T.T. & Chatterjee, A. Inter-cluster distance dependence of Electrical Conduction in Nanocluster Assembled Films of Silver: a new paradigm for designing of nanostructures. *Sci. Rep.* **5**, 7685; DOI:10.1038/srep07685 (2015).



This work is licensed under a Creative Commons Attribution-NonCommercial-NoDerivs 4.0 International License. The images or other third party material in this article are included in the article's Creative Commons license, unless indicated otherwise in the credit line; if the material is not included under the Creative Commons license, users will need to obtain permission from the license holder in order to reproduce the material. To view a copy of this license, visit <http://creativecommons.org/licenses/by-nc-nd/4.0/>